

T. Okubo
M. Suda

Alternate sign reversal in the ζ potential and synchronous expansion and contraction in the absorbed multi-layers of poly(4-vinyl-*N-n*-butylpyridinium bromide) cations and poly(styrene sulfonate) anions on colloidal silica spheres

Received: 12 January 1999
Accepted in revised form: 25 March 1999

Abstract Alternative multiple absorbed layers of up to ten macrocations [poly(4-vinyl-*N-n*-butylpyridinium bromide)] and macroanions [sodium poly(styrene sulfonate)] are formed on colloidal silica spheres above the critical concentration of macroions, m^* . The m^* value is the minimum number of macroions required to reverse the sign of the ζ potential of the spheres in the first absorption step. Alternate sign reversal in the ζ potential and expansive–contractive thickness changes are observed by the repeated and alternate addition of macrocations first and macroanions next. During multiple absorption, the pH and conductivity values decrease and increase continuously as the number of absorbed layers increases. When the macroanions are added

first, sign reversal in the ζ potential and reversible expansion and contraction do not occur. Breaking of the alternate multiple-type absorption occurs when equivalency in the number of dissociative groups of macrocations and macroanions is broken. Synchronous conformational changes of macrocations and macroanions in the multiple-absorbed layers, where balancing of the conformational rigidities with the multiple electrostatic attraction and repulsion between macrocations and anions occurs, are supported strongly.

Key words Synchronous absorption · Multiple absorption · Colloidal silica spheres · Electrophoretic measurement · Dynamic light scattering

T. Okubo (✉) · M. Suda
Department of Applied Chemistry
Faculty of Engineering
Gifu University, Yanagido 1-1
Gifu 501-1193, Japan
Tel.: +81-58-2932620

Introduction

In our previous work [1, 2] the abrupt sign reversal in the ζ potential of a colloidal sphere, usually negatively charged in the surface, was observed by the addition of various kinds of oppositely charged macroions and their low valency simple ions such as calcium and lanthanum ions. This suggests that the excess number of macroions compared to the number of charges on the colloidal surfaces are absorbed in the manner of the so-called avalanche-type synchronous absorption mechanism, i.e., absorption of macroions occurs abruptly on the colloidal surfaces above the critical concentration (m^*) of

macroions added. Below the critical concentration absorption does not occur so significantly.

It is possible to obtain multilayered absorption of macroions on the surface of anionic colloidal spheres by the addition of macrocations first, then macroanions, further macrocations, macroanions, and so on. This alternate absorption should occur through the electrostatic attraction between the absorbed colloidal spheres and the oppositely charged macroions. This report is the first one from our laboratory on the alternate changes in the charge sign and also in the thickness of the absorbed layer observed for macroion–colloidal complex systems.

We should note here that a similar layer-by-layer absorption of oppositely charged molecules including polymers has been studied intensively by Decher and coworkers [3–6]. They observed the reversible thickness changes in the absorbed layers. Several types of multiple absorption of macromolecules have been investigated hitherto [7–18]. Quite recently, multilayered cationic particles of rhodamine B-labeled melamine formamide with sodium poly(styrene sulfonate) (N-PSS) and poly(allylamine hydrochloride) were prepared and their Förster resonance energy transfer was discussed [19]. Furthermore, the ζ potential showed a nice alternate sign reversal of the spheres, though the thickness of the absorbed layers was not measured.

Experimental

Materials

The CS91 colloidal silica spheres were a gift from Catalyst & Chemicals Ind. (Tokyo). The diameter (d_0), the standard deviation (δ) from the mean diameter and the polydispersity index (δ/d_0) were 110 nm, 4.5 nm and 0.041, respectively. These size parameters were determined with an electron microscope. The charge density of the strongly acidic groups was $0.48 \mu\text{C}/\text{cm}^2$. NaPSS (molecular weight = 18000, polydispersity index $M_w/M_n = 1.14$) was obtained from Pressure Chemicals (Pittsburgh, Pa.). The details of the preparation and purification of poly-4-vinyl-*N*-*n*-butyl pyridinium bromide (C4PVP) was described in previous papers [20, 21]. The degree of polymerization of the parent polymer, poly-4-vinylpyridine was determined by viscometry to be 3800. The water used for the purification and suspension preparation was purified by a Milli-Q reagent grade system (Milli-RO5 plus and Milli-Q plus, Millipore Co., Bedford, Mass.).

Electrophoretic light-scattering measurements

ELS measurements were made on a Leza-600 ELS Zeta-meter (Otsuka Electronics, Osaka) at $25 \pm 0.02^\circ\text{C}$.

pH measurements

pH values of the sample suspensions were measured on a Beckman (Tokyo) model $\phi 34$ pH meter, with a glass electrode (model 6378-10D, Horiba, Kyoto) at $25 \pm 0.5^\circ\text{C}$.

Conductivity measurements

The conductivity of the suspension was measured on a model DS-14 conductivity meter (Horiba, Kyoto) with an electrode (no. 3552, Horiba) at $25 \pm 0.5^\circ\text{C}$.

Results and discussions

The ζ potential and the effective thickness of the absorbed layers in the macroion–colloid complex formed by the alternate addition of C4PVP first and

NaPSS on CS91 spheres are shown in Fig. 1. Here, the equivalent ionic concentrations were 8×10^{-6} monomol for both C4PVP and NaPSS polymers. Sphere concentrations were 7×10^{-5} in volume fraction and 5.2×10^{-9} Eq/l in equivalent concentration of the sphere charges. The critical concentration (m^*) of C4PVP for the charge reversal of CS91 spheres was 3×10^{-6} monoM [2]. The ζ potential repeated sign reversal beautifully. The small and large circles show the two runs of the ζ potential measurements and their mean values, respectively. The reproducibility of the ζ potential was excellent. Surprisingly, the thickness of the absorbed layers estimated from the ELS measurements also repeatedly expanded and shrank when the effective charges of the spheres were positive and negative, respectively. In this figure, two runs of the ELS measurements and their mean values are shown by the small and large triangles, respectively. The reproducibility of the thickness was not so good compared with that of the ζ potential, especially for more than seven layers.

It should be mentioned that the first absorption step is clearly avalanche-type, i.e., absorption of the macrocations occurred abruptly above the critical concentration of melting ($m^* = 3 \times 10^{-6}$ monoM), which is a great-excess compared with the equivalent concentration of sphere charges (5.2×10^{-9} Eq/l). Simple calculation tells us that 13 macrocations (degree of polymerization = 3800) are bound on a colloidal sphere in the first absorption step. Thus C4PVP molecules must be bound quite loosely on the colloidal surface, since the absorption layer of macrocations is very thick, about 400 nm. The contour length of C4PVP is estimated to be $950 \text{ nm} [0.25 \text{ nm}(\text{monomer length}) \times 3800(\text{degree of polymerization})]$, and the ionic concentration of the macrocations is $580 (3 \times 10^{-6} / 5.2 \times 10^{-9})$ times

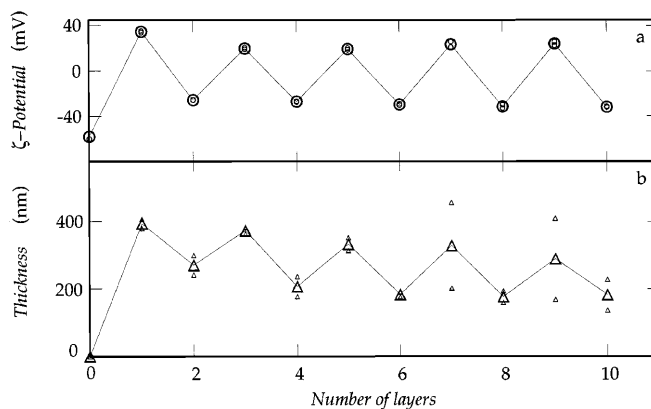


Fig. 1 **a** ζ potential and **b** absorbed layer thickness of CS91 spheres at 25°C . Poly-4-vinyl-*N*-*n*-butyl pyridinium bromide (C4PVP) (8×10^{-6} monoM) and sodium poly(styrene sulfonate) (NaPSS) (8×10^{-6} monoM) are added alternately: $\phi = 7 \times 10^{-5}$. Large symbols indicate the mean of the two runs shown by the small symbols

higher compared with that of the colloidal spheres. Therefore, it is highly plausible that one end of the macroions is bound on the colloidal surfaces with tail-type absorption and almost all of the macrocations are highly stretched in the suspension containing no foreign salt.

It should be further mentioned here that almost all the macroions are bound on the colloidal surfaces in each absorption step and that the numbers of free macrocations, macroanions and/or macrocation–macroanion complexes are negligibly small.

Figure 2 shows a schematic representation of the alternate multiple absorption of macrocations and macroanions on the colloidal surfaces speculated from the experimental results on the ζ potential and the thickness of the absorbed layers shown in Fig. 1. Expansion and contraction of the absorbed layers suggests several things. First, C4PVP molecules are bound more loosely than NaPSS. The rigidity of the polymer chain of the former is greater than that of the latter. The bulky *N*-butyl pyridinium moieties are the main reason for the difficulty of compact stacking. Second, the most outside absorbed layer is loosely bound and expanded compared with the inner layers, since the thickness of the first absorbed layer increases sharply to about 400 nm as shown in Fig. 1. Thirdly, synchronous balancing between the electrostatic attractions among the multiple interlayers of macrocations (e.g., *n*-valent) and anions (o-valent) accompanied with the polymer chain contraction and the electrostatic repulsions with the chain expansion within the intralayers. The third factor should be the synchronous and cooperative interactions among the *m*-valent silica surfaces and the absorbed layers of the macroions having ionic valencies of *n*+ and o−. Consider a ten-layered sphere with macrocations and macroanions, for example. First, the electrostatic attractive and repulsive

interactions among the 11 layers such as $[m+]-[n+]-[o-]-[n+]-[o-]-[n+]-[o-]-[n+]-[o-]-[n+]-[o-]$ must be taken account. Secondly, intralayer electrostatic repulsion may contribute to the synchronization. Third, nonelectrostatic (e.g., hydrophobic, dipole–dipole) inter- and intra-layered attractive interactions are important. Thirdly, the flexibilities of the macrocations and macroanions are important for the expansion forces in the intralayers. Theoretical consideration, where these factors are taken into account, is essential for understanding the synchronous nature of the absorption found in this work.

The pH and the conductivity of the complex suspensions in the course of the alternate absorption processes are shown in Fig. 3. Interestingly, the former decreased slightly and continuously, and the latter increased significantly and also continuously. The repeated expansion and contraction in the absorbed layers observed in Fig. 1 did not affect these two parameters so much.

The ζ potential (curves a) and the absorbed layer's thickness (b) when the NaPSS macroanions were added first to the suspension of the anionic colloidal silica spheres are shown in Fig. 4. Clearly, weak absorption occurs; however, no clear-cut alternate changes were observed in the ζ potential. The potentials remained negative at about −40 mV except for the first absorption step (−62 mV). This suggests the importance of the dipole–dipole attractive forces between the macroions and the colloidal spheres, especially in the first absorption step [2]. Interestingly, the thickness increased linearly though a slight reflection was observed in the curve of the plots of thickness against number of layers.

We should mention here that the order of addition of macroions and the equivalency in the ionic concentrations among colloidal spheres, macrocations and macroanions are highly important for the alternate multiple absorption. When macroanions are added first, a large

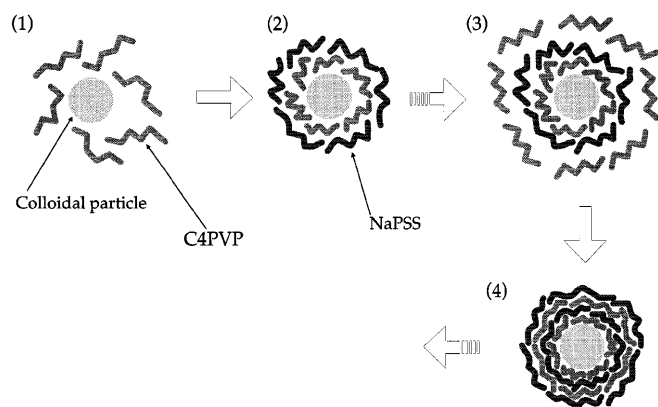


Fig. 2 Schematic presentation of multiple absorption of macrocations and macroanions on the colloidal surface

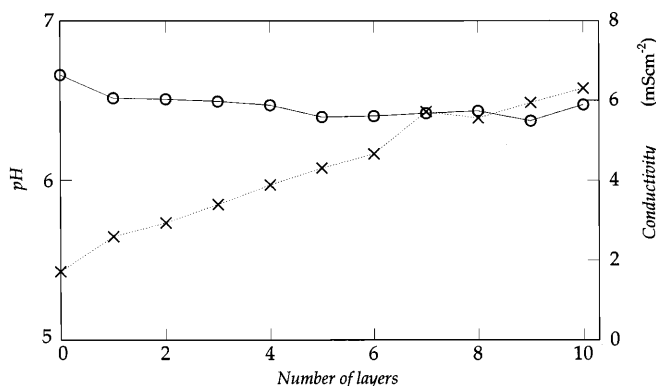


Fig. 3 pH (○) and conductivity (X) of CS91 spheres at 25 °C. C4PVP (8×10^{-6} monoM) and NaPSS (8×10^{-6} monoM) are added alternately: $\phi = 7 \times 10^{-5}$, NaPSS first

number of free macroanions coexist in suspension, and the macrocation and macroanion complexes are also formed in the addition processes.

Figure 5 shows the ζ potential and the thickness of the absorbed layer when the concentrations of both C4PVP and NaPSS are 10^{-6} monoM, i.e., below the critical concentration of the charge reversal ($m^* = 3 \times 10^{-6}$ Eq/l). Clearly, the alternate change in the sign of the ζ potentials was not observed irrespective of the kind of macroions added in the first step; however, the thickness of the absorbed layers increased slightly as the number of layers increased.

The ζ potential and the thickness of the absorbed layer when the concentrations of C4PVP and NaPSS are below and above the critical concentration respectively, are shown in Fig. 6. Fluctuations in the two parameters were vague except for the first few processes. It should be noted that the absorption took place in the first few

steps. The results suggest that the equivalency of the charges between the macrocations and macroanions is important for the alternate sign reversal in the ζ potential and the synchronous expansion and contraction in the absorbed layers.

Figure 7 shows the ζ potential and the thickness of the absorbed layer when the concentrations of C4PVP and NaPSS are above and below the m^* value, respectively, i.e., the opposite condition to that in Fig. 6. When C4PVP was added first, the second and the following processes did not show any significant increase in the thickness, and the ζ potential returned to that of the bare silica spheres. It should be noted that an increase in the thickness of the absorption layers was observed even when the equivalency was broken as shown in Figs. 6 and 7.

The data presented in Figs. 4–7 clearly suggest that the alternate sign reversal in the ζ potential and the

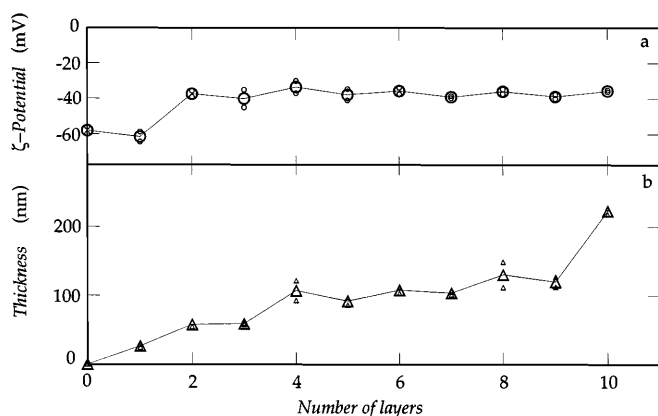


Fig. 4 **a** ζ potential and **b** absorbed layer thickness of CS91 spheres at 25 °C. C4PVP (8×10^{-6} monoM) and NaPSS (8×10^{-6} monoM) are added alternately: $\phi = 7 \times 10^{-5}$, NaPSS first, *Large symbols* indicate the mean of the two runs shown by the *small symbols*

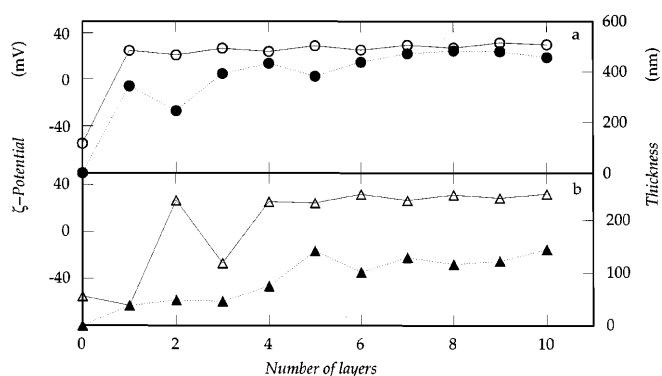


Fig. 6a, b ζ potential (\circ , \triangle) and absorbed layer thickness (\bullet , \blacktriangle) of CS91 spheres at 25 °C. C4PVP (1.6×10^{-5} monoM) and NaPSS (8×10^{-6} monoM) are added alternately: $\phi = 7 \times 10^{-5}$, **a** C4PVP first, **b** NaPSS first

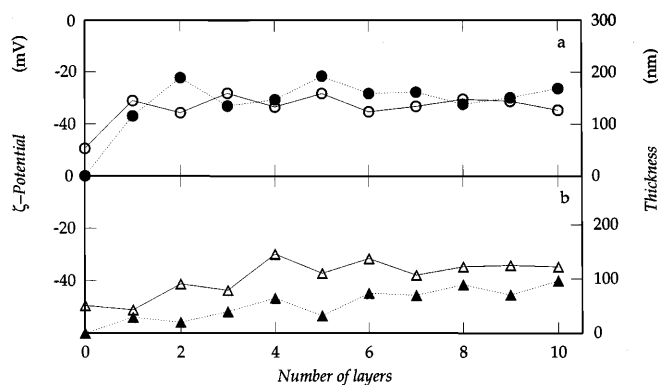


Fig. 5a, b ζ potential (\circ , \triangle) and absorbed layer thickness (\bullet , \blacktriangle) of CS91 spheres at 25 °C. C4PVP (10^{-6} monoM) and NaPSS (10^{-6} monoM) are added alternately: $\phi = 7 \times 10^{-5}$, **a** C4PVP first, **b** NaPSS first

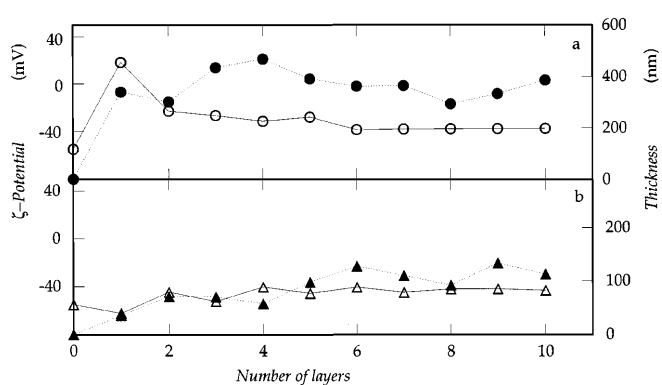


Fig. 7a, b ζ potential (\circ , \triangle) and absorbed layer thickness (\bullet , \blacktriangle) of CS91 spheres at 25 °C. C4PVP (8×10^{-6} monoM) and NaPSS (1.6×10^{-5} monoM) are added alternately: $\phi = 7 \times 10^{-5}$, **a** C4PVP first, **b** NaPSS first

expansion and contraction in the thickness of the absorbed layer shown in Fig. 1 only occur when 1. The macrocation is added first. 2. The ionic concentrations of macrocations and macroanions are equivalent. 3. The concentrations of the macroions are above the m^* value.

Balancing of the electrostatic, hydrophobic and dipole–dipole interactions between the colloidal spheres and the macroions must be important for the synchro-

nous expansion and contraction. The theoretical aspects of this unique absorption phenomenon are quite important and are now being investigated in our laboratory with further systematic experimental studies.

Acknowledgements Financial support from the Ministry of Education and Culture, Japan is acknowledged. M. Komatsu and M. Hirai of Catalysts & Chemicals Ind. (Tokyo and Kitakyusyu) are thanked for providing the silica sphere sample.

References

- Okubo T (1990) *Polym Bull* 23:211
- Okubo T, Suda M (1999) *J Colloid Interface Sci* 213:565
- Decher G, Hong JD (1991) *Makromol Chem Symp* 46:321
- Decher G, Hong JD (1991) *Ber Bunsenges Phys Chem* 95:1430
- Decher G, Hong JD, Schmitt J (1992) *Thin Solid Films* 210/211:831
- Sukhorukov GB, Schmitt J, Decher G (1996) *Ber Bunsenges Phys Chem* 100:948
- Schmitt J, Grunewald T, Kjaerk K, Pershan P, Decher G, Losche M (1993) *Macromolecules* 26:7058
- Decher G, Lvov Y, Schmitt J (1994) *Thin Solid Films* 244:772
- Decher G, Lehr B, Lowack K, Lvov Y, Schmitt J (1994) *Biosens Bioelectron* 9:677
- Ferreira M, Cheung JH, Rubner MF (1994) *Thin Solid Films* 244:806
- Gao M, Zhang X, Yang Y, Yang Y, Yang B, Shen J (1994) *J Chem Soc Chem Commun* 2777
- Kleinfeld ER, Ferguson GS (1994) *Science* 265:370
- Keller SW, Kim HN, Mallouk TE (1994) *J Am Chem Soc* 116:8817
- Kong W, Zhang X, Gao ML, Zhou H, Li W, Shen JC (1994) *Macromol Rapid Commun* 15:405
- Korneev D, Lvov Y, Decher G, Schmitt J, Yaradaikin S (1995) *Thin Solid Films* B 213/214:954
- Onoda M, Yoshino K (1995) *Jpn J Appl Phys* 34:L260
- Savami F, Maassen E, Tieke B, Jordan G, Rammensee W (1995) *Langmuir* 11:1068
- Lvov Y, Ariga K, Kunitake T (1995) *Am Chem Soc* 117:6117
- Caruso F, Donath E, Mohwald H (1998) *J Phys Chem* 102:2016
- (a) Okubo T, Ise N (1973) *J Am Chem Soc* 95:2293; (b) Okubo T, Ise N (1973) *J Am Chem Soc* 95:4031
- Ishiwatari T, Okubo T, Ise N (1980) *Polym Sci* 18:1807